



# THE UNIVERSITY *of* EDINBURGH

## Edinburgh Research Explorer

### Modeling expanded perlite production in a vertical electrical furnace

**Citation for published version:**

Angelopoulos, P, Gerogiorgis, D & Paspaliaris, I 2013, 'Modeling expanded perlite production in a vertical electrical furnace'. in I Nishkov, I Grigorova & D Mochev (eds), Proceedings of the 25th Balkan Mineral Processing Congress & Exhibition. Publishing House "St. Ivan Rilski", SOZOPOL, pp. 695-701.

**Link:**

[Link to publication record in Edinburgh Research Explorer](#)

**Document Version:**

Publisher final version (usually the publisher pdf)

**Published In:**

Proceedings of the 25th Balkan Mineral Processing Congress & Exhibition

**General rights**

Copyright for the publications made accessible via the Edinburgh Research Explorer is retained by the author(s) and / or other copyright owners and it is a condition of accessing these publications that users recognise and abide by the legal requirements associated with these rights.

**Take down policy**

The University of Edinburgh has made every reasonable effort to ensure that Edinburgh Research Explorer content complies with UK legislation. If you believe that the public display of this file breaches copyright please contact [openaccess@ed.ac.uk](mailto:openaccess@ed.ac.uk) providing details, and we will remove access to the work immediately and investigate your claim.



# MODELING EXPANDED PERLITE PRODUCTION IN A VERTICAL ELECTRICAL FURNACE

Panagiotis M. Angelopoulos<sup>1</sup>, Dimitrios I. Gerogiorgis<sup>2</sup> and Ioannis Paspaliaris<sup>3</sup>

<sup>1,2,3</sup> School of Mining and Metallurgical Engineering, National Technical University of Athens, GR-15780 Athens, Greece  
E-mail: <sup>1</sup> [pangelopoulos@metal.ntua.gr](mailto:pangelopoulos@metal.ntua.gr), <sup>2</sup> [dgerogiorgis@metal.ntua.gr](mailto:dgerogiorgis@metal.ntua.gr), <sup>3</sup> [paspali@metal.ntua.gr](mailto:paspali@metal.ntua.gr).

**ABSTRACT.** Expanded perlite has outstanding thermal and acoustic insulating properties and is widely used in the manufacturing and construction industries. The conventional perlite expansion method has certain disadvantages which affect the quality of expanded perlite products, thus limiting their performance and range of applications. A new perlite expansion process has been designed and a vertical electrical furnace for perlite expansion has been constructed in our laboratory in order to overcome these drawbacks, enabling precise control of experimental conditions in order to prescribe the temperature profile and residence time within the new heating chamber. A novel dynamic model for perlite grain expansion has been developed and validated so as to study and optimize the new furnace operation. Perlite ore origin, size distribution and water content are key parameters affecting expanded perlite quality. Moreover, air feed flow rate and temperature, as well as the imposed wall temperature distribution along the heating chamber are experimentally known to have a profound, measurable effect on grain residence time and expansion. A detailed sensitivity analysis has been performed so as to quantitatively understand the effect and relative importance of all foregoing operational parameters on macroscopic furnace operation (perlite particle velocity and temperature evolution) as well as on inaccessible microscopic characteristics (internal steam bubble pressure and size). Perlite grain radius and expansion ratio are probed in detail as a function of time, and furnace operation can be tuned vs. feed variation toward optimal product quality. Particle critical characteristics along trajectories as well as final particle size plots are presented; also, optimal furnace operating condition ranges are determined for variable initial size and water content.

**Keywords:** Perlite expansion, vertical electrical furnace, dynamic modeling, process simulation, sensitivity analysis.

**Relevant Congress Topics:** Simulation, Control & Modeling in Mineral Processing, Processing of Industrial Minerals.

## INTRODUCTION

Perlite is a natural occurring volcanic siliceous rock which consists mainly of amorphous silica (70-76 % wt.) but also contains smaller quantities of numerous other metal oxides ( $\text{Al}_2\text{O}_3$ ,  $\text{K}_2\text{O}$ ,  $\text{Na}_2\text{O}$ ,  $\text{Fe}_2\text{O}_3$ ,  $\text{CaO}$ ,  $\text{MgO}$ ). Perlite can be expanded from 4 to 20 times its original volume when heated at a temperature close to its softening point (700-1260 °C), due to the presence of 2-6% chemically bound water within its microstructure (Chatterjee, 2008). Conventional perlite expansion is usually accomplished by feeding ground, pre-sized perlite ore into a vertical furnace heated by a direct gas flame at its bottom end, thus directing forced air flow upwardly: ore particles are typically introduced into the hottest expansion chamber region, near the flame, at a temperature of ca. 1450 °C. During expansion, perlite acquires outstanding physical properties (low density, thermal and acoustic insulation) which render it suitable for many applications in the construction and manufacturing industries. The currently prevalent perlite expansion process is the only globally reliable production technology: although the method has been in continuous use for more than 50 years, it remains a largely empirical industrial process, despite the rapid increase and proliferation of expanded perlite uses and applications over the past few decades. Its main technical problems include: (1) the high heat losses due to the off-gas stream which in turn cause high energy consumption, and (2) the violent, poorly controlled heating of raw feed in conventional furnaces, producing expanded material with unfavourable mechanical properties and adversely affecting the quality and range of perlite applications.

To overcome these serious drawbacks, a new perlite expansion process has been designed and a new pilot-scale production unit has been constructed, based on the idea of a vertical, electrically heated expansion furnace.

The new vertical electrical furnace has been designed for maximizing experimental flexibility, in order to facilitate the adjustment of operating conditions versus raw material but also final product quality specifications. The new perlite expansion method allows the milder, gradual heating of perlite grains, but also facilitates the variation of perlite particle residence time in the heating chamber. Experimental perlite expansion campaigns conducted on this pilot-scale production unit indicate a remarkable improvement and a definite operating cost reduction in expanded perlite properties compared with conventional processing. Hence, the multi-parametric mathematical investigation of the process system thermal behavior and the identification of the effect of all crucial operational parameters on perlite expansion dynamics is an endeavor of evident importance which must guide the optimization of the entire experimental pilot-scale facility as well as every subsequent production-scale process. Investigating the effect of key operational parameters on product quality yields profound process understanding.

## THE VERTICAL ELECTRICAL FURNACE

The vertical electrical perlite expansion furnace consists of the air preheater and flow control system, the perlite feeding system, the heating chamber and the furnace temperature control system (Figure 1). Atmospheric air is introduced into the system by an air compressor and the volumetric flow rate is measured and controlled by a dedicated system of flowmeters and valves. The air is injected at the top of the furnace through six 0.009 m diameter holes located symmetrically around the perlite inlet hole and at a distance of 0.044 m from the center. Air can be heated via a preheater which has a heat capacity of 2 kW, raising temperature up to ca. 500 °C. The desirable perlite feeding rate is achieved by a rotary

air-lock feeder, through a 0.08 m diameter central hole. The rotary air-lock feeder prevents hot air upward drafts but also the escape of perlite particles from the furnace. The cylindrical heating chamber is 3 m long and 0.134 m wide, and is made of Kanthal APM FeCrAl alloy. The chamber is heated by 6 pairs of electrical resistances located along the tube, defining six heating zones. Each pair consists of two semicylindrical Kanthal resistances, located against each other around the chamber and at a distance of about 3 cm out of it, providing a total heating capacity of 24 kW to the expansion process. The chamber and resistances are encased in a cylindrical aluminosilicate insulation case of 0.165 cm thickness. Temperature measurements in each zone are obtained by a ceramic sheathed K-type thermocouple (NiCr/NiAl) placed at each zone center, and air inlet temperature is measured by a thermocouple before the head. Preheater and all zone temperatures are all individually controlled.

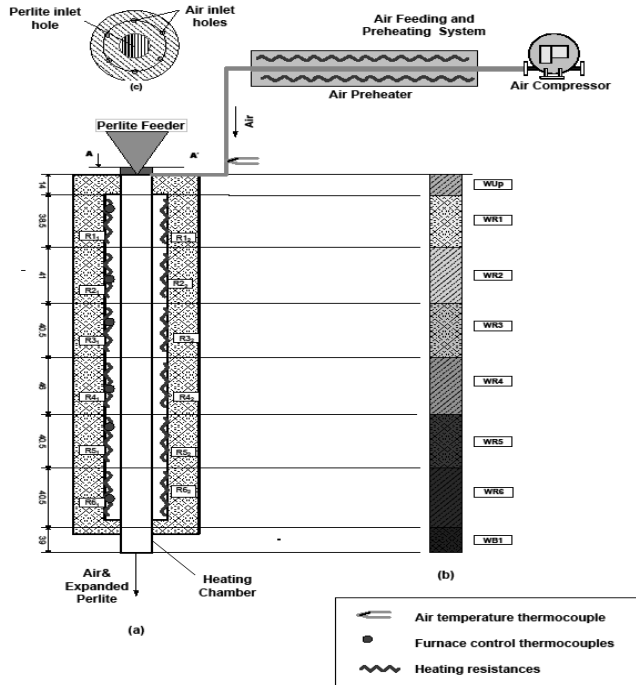


**Figure 1. Schematic of the experimental installation for perlite expansion, illustrating all vertical electrical furnace heating zones and its auxiliary systems.**

## AIR AND PERLITE PROPERTIES

### Air Thermophysical Properties

Air can be injected into the heating chamber at a temperature of 25 °C and heated up to 1200 °C: property variations can hence be dramatic, so incorrect estimates induce significant error in energy balances. Air density variation affects the volumetric air flow rate along the vertical heating chamber, inducing an increase of superficial air velocity; it also affects the buoyancy and drag forces in the perlite grain momentum balance and the convective heat transfer rate from air to each particle. Air density variation along the heating chamber due to temperature increase is calculated by the ideal gas law:

$$\rho_{air} = \frac{P}{R_g T_{air}} \quad (1)$$

Here,  $\rho_{air}$  is the air density ( $\text{kg}\cdot\text{m}^{-3}$ ),  $R_g$  is the ideal gas law constant and pressure is taken constant ( $P = 1 \text{ atm}$ ).

Air viscosity is calculated by means of the next equation:

$$\mu_{air} = \mu_{air,ref} \left( \frac{T_{air}}{T_{air,ref}} \right)^{n_{ref}} \quad (2)$$

The parameter values for air viscosity calculation here are:  $\mu_{air,ref} = 1.72 \cdot 10^{-5} \text{ Pa}\cdot\text{s}$ ,  $T_{air,ref} = 273 \text{ K}$  and  $n_{ref} = 0.7$ .

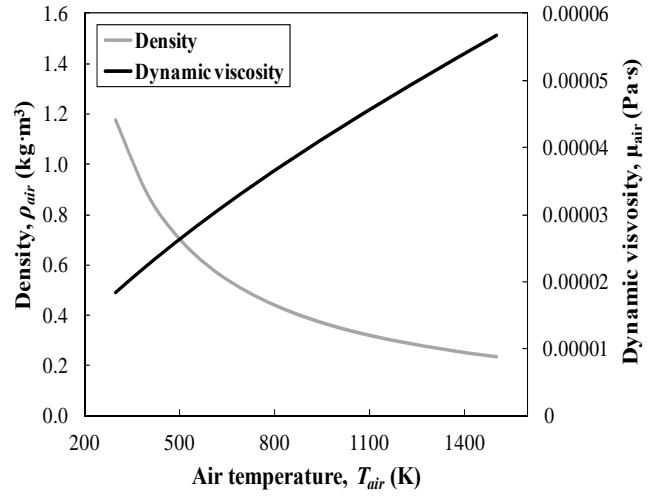


**Figure 2. Air density ( $\rho_{air}$ ) and dynamic viscosity ( $\mu_{air}$ ) vs. temperature, calculated by Equations (1) and (2).**

Air heat capacity under constant pressure as well as air thermal conductivity can be calculated using polynomials:

$$C_{p,air} = \alpha_{Cp,1} T_{air}^3 + \alpha_{Cp,2} T_{air}^2 + \alpha_{Cp,3} T_{air} + \alpha_{Cp,4} \quad (3)$$

The coefficient values for  $\alpha_{Cp,1}$ ,  $\alpha_{Cp,2}$ ,  $\alpha_{Cp,3}$ , and  $\alpha_{Cp,4}$  are:  $-8.01440 \cdot 10^{-8}$ ,  $2.10788 \cdot 10^{-4}$ ,  $2.06329 \cdot 10^{-2}$ ,  $9.83672 \cdot 10^2$ .

$$k_{air} = \alpha_{k,1} T_{air}^3 + \alpha_{k,2} T_{air}^2 + \alpha_{k,3} T_{air} + \alpha_{k,4} \quad (4)$$

Similarly, the coefficient values for  $\alpha_{k,1}$ ,  $\alpha_{k,2}$ ,  $\alpha_{k,3}$ ,  $\alpha_{k,4}$  are:  $-1.5207 \cdot 10^{-11}$ ,  $-4.8574 \cdot 10^{-8}$ ,  $1.0184 \cdot 10^{-4}$  and  $-3.9333 \cdot 10^4$ .

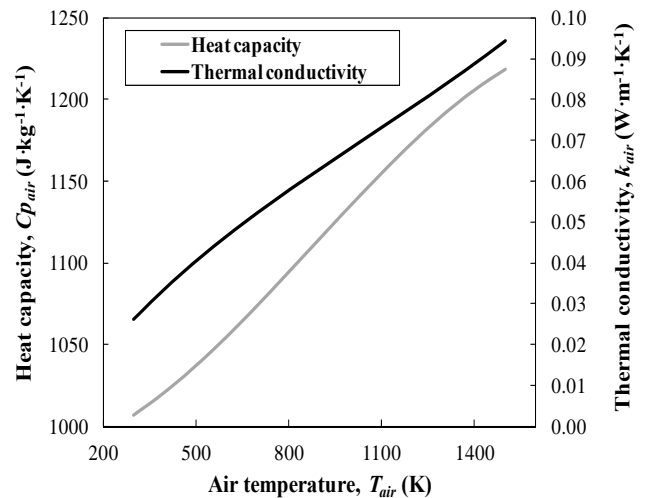


**Figure 3. Air heat capacity and thermal conductivity vs. temperature, calculated by Equations (3) and (4).**

Figures 2 and 3 present all air thermophysical properties ( $\rho_{air}$ ,  $\mu_{air}$ ,  $C_{p,air}$ ,  $k_{air}$ ) versus absolute temperature in the entire process range, illustrating their significant variation.

## Perlite Melt Thermophysical Properties

In our research we investigated perlite ore particles obtained from the Trachilas mine which is located in the island of Milos, Greece. The perlite ore considered in this modeling study consists of amorphous silica (73% wt. SiO<sub>2</sub>), aluminium oxide (12.7% Al<sub>2</sub>O<sub>3</sub>), other metal oxide amounts (K<sub>2</sub>O, Na<sub>2</sub>O, Fe<sub>2</sub>O<sub>3</sub>, CaO) and 3.32 % LOI (Lost On Ignition) matter. Water plays the most important role in the entire expansion process, not only by expanding the grain during evaporation but also by reducing the viscosity of the softened grain shell; the amount of perlite water which is available and responsible for its potential to expand on heating has been studied by previous publications (King et al. 1948; Shackley, 1988). Based on LOI tests, we conclude that a water portion remains in the expanded grain without participating in expansion: this is the *residual water* (40%) which is only considered in perlitic melt thermophysical property calculation, while the remaining *effective water* (60%) drives steam bubble growth and perlite grain expansion. Perlite melt density is assumed constant ( $\rho_m = 2300 \text{ kg}\cdot\text{m}^{-3}$ ) in the entire grain temperature range; Zahringer *et al.* used a mean value of  $2350 \text{ kg}\cdot\text{m}^{-3}$ , while Proussevitch *et al.* used a rhyolitic melt density of  $2200 \text{ kg}\cdot\text{m}^{-3}$  (Proussevitch and Sahagian, 1988; Zahringer et al., 2001). Our raw perlite ore density measurement ( $2290 \text{ kg}\cdot\text{m}^{-3}$ ) agrees with literature values.

Perlite expansion evolution is affected by molten grain shell viscosity, which varies significantly during the process and is a strong nonlinear temperature function: a recent study considers compositional and heat effects on magmatic liquid viscosity, developing a multi-parametric algebraic model which we have adopted here in order to calculate perlite melt viscosity as a function of chemical composition and temperature (Giordano et al., 2008). The temperature dependence of viscosity is modeled by the Vogel-Fulcher-Tammann (VFT) equation, where J, X and Y (pre-exponential factor, pseudo-activation energy and VFT temperature, respectively) are given via correlations:

$$\log \mu_m = J + \frac{X}{T_m - Y} \quad (5)$$

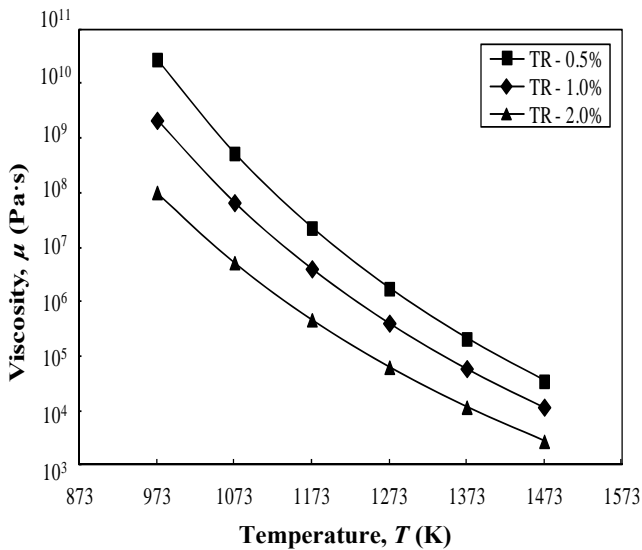


**Figure 4. Melt viscosity temperature variation for the Trachilas melt chemical composition (TR) and three water content values ( $w_{H_2O} = 0.5, 1, 2\%$ ), calculated by means of a literature model (Giordano et al., 2008).**

Melt viscosity decreases dramatically as temperature rises: in the temperature range of 297-973 K, viscosity is very high and hinders particle expansion completely, as seen in the bubble radius equation (26) (thus not shown). The water content of the melt is a key parameter affecting melt viscosity, as we confirmed by the Giordano model: a mere 1% increase in perlitic melt water content induces a decrease of melt viscosity which is higher than a whole order of magnitude, as evidently illustrated in Figure 4. The nonlinear sensitivity of viscosity has a dramatic effect on perlite expansion which is confirmed by model results.

The surface tension on the shell-bubble interface ( $\sigma$ ) is also critical, because it counteracts bubble expansion. The temperature dependence of perlitic melt surface tension can be approximated by a linear correlation which is published for the similar obsidian melt (0.5% wt. H<sub>2</sub>O). The next equation used for surface tension calculation is valid in the 1000-1400 °C range (Zahringer et al., 2001):

$$\sigma = 1.971 \cdot 10^{-4} T_m + 0.09317 \quad (6)$$

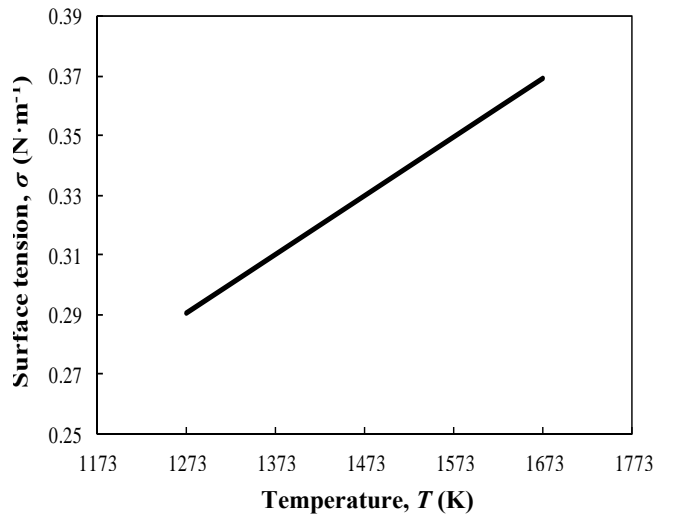


**Figure 5. Melt surface tension temperature variation for obsidian, a similar material (Zahringer et al., 2001).**

Figures 4 and 5 present melt thermophysical properties ( $\mu$  and  $\sigma$ , respectively) versus absolute temperature in the key process range, illustrating considerable variation.

Perlite melt heat capacity under constant pressure is another critical property which affects the heat balance. King et al. (1948) have proposed the following equation for the estimation of anhydrous perlite heat capacity:

$$C_{P,ap} = 41.868 \cdot (24.25 + 4.66 \cdot 10^{-3} T - 6.62 \cdot 10^{-5} T^{-2}) \quad (7)$$

The specific heat capacity of the steam as a function of temperature is calculated using the following linear correlation (Gordon and Barnes, 1932; Gordon, 1934):

$$C_{P,H_2O} = 0.6417 \cdot T + 1646.9 \quad (8)$$

The effective particle heat capacity has been calculated as a function of particle perlite and water mass fractions, to explicitly consider its considerable process variation. The overall heat capacity of the two-phase perlite particle is thus calculated by the next equation in terms of both particle temperature and effective water mass fraction:

$$C_{P,p} = w_{H_2O,eff} \cdot C_{P,H_2O} + (1 - w_{H_2O,eff}) \cdot C_{P,ap} \quad (9)$$

## THE MATHEMATICAL MODEL

The dynamic mathematical model we have developed concentrates on the momentum and energy balance of single-grain expansion in the vertical electrical furnace, combining both a microscopic and a macroscopic level. Microscopic mathematical analysis here refers to the investigation of internal particle temperature and steam bubble pressure evolution, as the interplay and rates of both these phenomena governs perlite grain expansion. Macroscopic mathematical analysis here refers to particle motion (force balance) and air temperature distribution. These transport phenomena are analyzed via a nonlinear system of algebraic and ordinary differential equations.

### Dynamic Mathematical Modeling Assumptions

The fundamental assumptions for the macroscopic and microscopic parts of the mathematical model are important in order to understand the scope and accuracy of the model as well as the limits of its applicability. Air is introduced through the entire face of the cylindrical chamber, without any pressure drop ( $P = 1$  atm): its temperature along the heating chamber has no radial variation, and the entire chamber wall surface is smooth. Air temperature and velocity distributions are studied via one-dimensional models, as radial air velocity is zero. The effect of air components which are not transparent to thermal radiation ( $\text{CO}_2$ ,  $\text{H}_2\text{O}$ ) is negligible and does not affect air heating. Each perlite grain is considered perfectly spherical throughout the expansion process and has a uniform temperature which varies during expansion only due to heating and evaporation phenomena. Diffusion or mass transfer across the bubble-shell and the shell-environment interface has not been considered. The entire amount of the effective water content within the perlite grain is concentrated at the steam bubble nucleus throughout the expansion process. Steam obeys the ideal gas law in the entire process. The enthalpy of water evaporation inside grains is explicitly considered, but mechanical work for bubble expansion is negligible.

### Perlite Particle Motion

The forces exerted on falling particle are the gravitational force ( $F_G$ ) which accelerates the particle, the buoyancy force ( $F_B$ ) and the drag force ( $F_D$ ) which decelerate the perlite grain vertical fall by continuously opposing motion:

$$F_G = m_p g \quad (10)$$

$$F_B = \rho_{air} g V_p \quad (11)$$

$$F_D = \frac{1}{2} \rho_{air} C_D A_{proj} (U_{air} - U_p)^2 \quad (12)$$

The momentum balance on the falling perlite particle follows Newton's 2<sup>nd</sup> law of mechanics: considering all forces exerted on a grain, particle velocity is calculated via a simple ODE equation (Morsi and Alexander, 1972):

$$\sum F = m_p \frac{dU_p}{dt} \Rightarrow \frac{dU_p}{dt} = \frac{\rho_p - \rho_{air}}{\rho_p} g - \frac{3}{4} \frac{\rho_{air} C_D (U_{air} - U_p)^2}{D_p \rho_p} \quad (13)$$

The particle drag force coefficient ( $C_D$ ) is calculated via its Reynolds number ( $Re_p$ ) (Schiller and Nauman, 1933):

$$C_D = \frac{24}{Re_p} (1 + 0.15 \cdot Re_p^{0.687}) \quad (14)$$

The particle Reynolds number ( $Re_p$ ) is calculated in the model using its relative velocity vs. air in the equation:

$$Re_p = \frac{\rho_{air} D_p |U_p - U_{air}|}{\mu_{air}} \quad (15)$$

The significant variation of volumetric air flow rate due to the increase of air temperature and the decrease of air density along the heating chamber is taken into account toward air velocity calculation, via the following equation:

$$U_{air} = \frac{\dot{Q}_{air,in} T_{air}}{A_{tube} T_{air,in}} \quad (16)$$

### Air Heat Balance

The problem of air temperature calculation in the heating chamber can be considered and solved as follows: air is injected into a vertical tube and flows at mean velocity, within heated furnace walls of constant temperature. Thermal energy is transferred to the air by convection, thereby causing a definite increase in the air temperature. Air temperature calculation is based on an adiabatic energy balance, with initial condition:  $T_{air}(z=0) = T_{air,in}$ .

$$\frac{dT_{air}}{dz} = \left( \frac{\pi D_t h}{\dot{m} C_{p,air}} \right) (T_w - T_{air}) \quad (17)$$

The convective heat transfer coefficient ( $h$ ) along the heating chamber is calculated by the following equation:

$$h = \frac{k_{air} Nu_{air}}{D_t} \quad (18)$$

The air Nusselt number is calculated by the Sieder-Tate equation for hydrodynamically/thermally developing flow:

$$Nu_{air} = 1.86 \cdot \left( \frac{Re \cdot Pr \cdot D_t}{z} \right)^{1/3} \left( \frac{\mu_{air}}{\mu_w} \right)^{0.14} \quad (19)$$

The hydrodynamically developing region length ( $L_{hyd}$ ) is calculated by the following equation (Cengel, 2006):

$$L_{hyd} = 0.05 \cdot Re \cdot D_t \quad (20)$$

The thermally developing region length ( $L_{th}$ ) can also be determined by the following equation (Cengel, 2006):

$$L_{th} = 0.05 \cdot Re \cdot Pr \cdot D_t \quad (21)$$

For fully hydrodynamically and thermally developed flow, the Nusselt number assumes the constant value of 3.66.

### Perlite Grain Energy Balance

The falling perlite grain is assumed to have a uniformly varying temperature, as internal gradients are negligible. The validity of this assumption is confirmed by a Biot number calculation ( $Bi$ ) for a compact unexpanded grain: for process conditions and all thermophysical properties therein, the  $Bi$  value never exceeds  $Bi_{max} = 0.047$ , even in the most unfavorable case of maximum resistance to conductive heating: as  $Bi_{max}$  is much lower than the limit value of  $Bi_c = 0.1$  (a case for which literature indicates that total radial temperature variation cannot exceed 5%), we conclude the uniform temperature assumption is valid.

The solid particle absorbs energy by radiation and convection: both contribute to heating and expansion and they are equally important heat transfer mechanisms in order to understand furnace as well as process efficiency. The grain temperature evolution due to radiative heating is calculated on the basis of the Stefan-Maxwell law, thus accounting for the thermal energy emitted by the furnace walls and absorbed by the moving perlite grain. Furthermore, the solid particle exchanges thermal energy with air by convective heating: this is an interesting phenomenon, as one can in fact numerically identify a sign reversal along the perlite grain trajectory: initially the cold particles are heated by the upward air current, but they are warmer than air as they approach the exit. Consequently, perlite grain temperature evolution is governed by the combination of radiative and convective heat transfer mechanisms and the dynamic heat balance is given by the following ordinary differential equation:

$$\frac{dT_p}{dt} = \varepsilon_p \cdot \frac{A_s s (T_w^4 - T_p^4)}{\rho_p V_p C_{p_p}} + \frac{A_s h_c (T_{air} - T_p)}{\rho_p V_p C_{p_p}} - \Delta H_{evap} \left( \frac{P_b}{R_g T_p} \right) \left( \frac{4\pi R_b^3}{3} \right) \quad (22)$$

Here,  $\varepsilon_p$  is the particle emissivity,  $A_s$  is the perlite particle surface area,  $s$  is the Stefan-Boltzmann constant and  $\Delta H_{evap}$  is the evaporation molar enthalpy (40.68 kJ·mol<sup>-1</sup>). The emissivity value for unexpanded and expanded perlite powder has been determined to be 0.7 and 0.55, respectively, according to measurements which we have conducted using an AE1 emissometer operated at NTUA. The model value changes as soon as expansion occurs.

### Steam Bubble Growth within the Perlite Grain

The present mathematical modeling study considers perlite expansion by means of a detailed single-grain model which idealizes a particle consisting of a spherical steam nucleus and a solid shell surrounding the bubble. Steam is treated as an ideal gas, with no mass transfer across the steam-shell or the shell-environment interface permitted. During grain heating, the temperature increase has a dual effect: steam enthalpy increases, increasing the pressure on the bubble-shell interface; concurrently, melt viscosity and cohesion decrease, facilitating bubble expansion and increasing bubble radius and grain size.

The pressure factors acting on the bubble-shell interface are the surface tension ( $\sigma$ ), the steam pressure ( $P_b$ ), and the ambient pressure ( $P_a$ ): steam pressure acts towards expanding the bubble, while both surface tension and ambient pressure act against steam bubble growth. The steam bubble only contains the entire effective water amount, since the residual water amount is uniformly dispersed in the molten shell without affecting expansion. The initial steam bubble radius ( $R_{b,i}$ ) can be calculated via a mass balance and the following cubic root equation:

$$R_{b,i} = \sqrt[3]{R_{p,i}^3 - \frac{3}{4\pi} \frac{m_m}{\rho_m}} \quad (23)$$

The molten shell mass ( $m_m$ ) is calculated using the grain water mass fraction ( $w_{H_2O}$ ) by the following equation:

$$m_m = (1 - w_{H_2O}) m_p \quad (24)$$

The steam in the core of the grain is treated as ideal gas; its instantaneous pressure is calculated by considering the bubble radius evolution in the bubble volume term and implementing the ideal gas law constitutive equation:

$$P_b(t) = \frac{3NR_g T_p}{4\pi R_b^3(t)} \quad (25)$$

The Navier-Stokes equation for spherical creeping flow is combined with the melt radial velocity equation and the bubble surface stress balance, to yield an ordinary differential equation for bubble radius evolution (Patel, 1980; Pai and Favelukis, 2002; Elshereef et al., 2010):

$$\frac{dR_b}{dt} = \frac{R_b}{4\mu_m} \left( P_b(t) - P_a - \frac{2\sigma}{R_b} \right) \quad (26)$$

The required initial condition is the miniscule steam bubble radius assumed at grain injection:  $R_b(t=0) = R_{b,i}$ .

## RESULTS AND DISCUSSION

A computer model has been developed to streamline the systematic numerical investigation of the process. The dynamic operation of the novel furnace is modeled using the Berkeley Madonna<sup>®</sup> ODE modeling platform (version 8.3.18), using a dual-core Intel Pentium T3200 (2 GHz) with 3 GB of RAM operating in Windows Vista (32-bit). The foregoing nonlinear system of algebraic and ordinary differential equations is solved via a 4<sup>th</sup>-order Runge-Kutta numerical integration, using solution and reporting timesteps of  $\Delta t_s = 0.01$  s and  $\Delta t_r = 0.05$  s, respectively.

The model computes the evolution of all particle state variables (bubble pressure, particle temperature, particle velocity, particle position, particle radius and expansion ratio) and the air temperature distribution in the furnace, enabling investigation of the perlite expansion method towards cost-effective optimization. Operating parameter (furnace wall temperature, air feed flow and temperature) and raw material physical property variations (initial size and water content) have been considered as dynamic model input parameters, to probe their significance and relative effect on expansion efficiency by quantitatively determining their individual effect on expansion ratio ( $E$ ).

Figure 6 presents temporal plots of all particle state variables for variable heating chamber wall temperatures and a water content of  $w_{H_2O,eff} = 2.00\%$  (Trachilas mine). Steam bubble pressure increases due to the temperature increase: a relief is observed at 600 °C, as shell viscosity and cohesion decrease and the bubble starts expanding. Particle temperature strongly depends on furnace wall temperature but also on heating chamber residence time. Particles decelerate rapidly at expansion onset, due to the strong impact of radius on drag and buoyancy forces: thus, expanded particle residence time is clearly longer. Fully expanded particles' and wall temperature coincide due to the prolonged lightweight particle residence time.

Figure 7 presents the effect of particle initial size and water content on final expansion ratio ( $E = R_{p,final} / R_{p,i}$ ). Preheated air injection in the heating chamber is vital for adequate perlite heating and expansion, providing a uniform driving force and thus enhancing controllability. While ambient air use implies heating beyond 1000 °C for adequate expansion ( $E > 2$ ), preheated air use allows for achieving much higher expansion ratios ( $2.5 < E < 5$ ) for most raw feed fractions, even at a temperature of 900 °C.

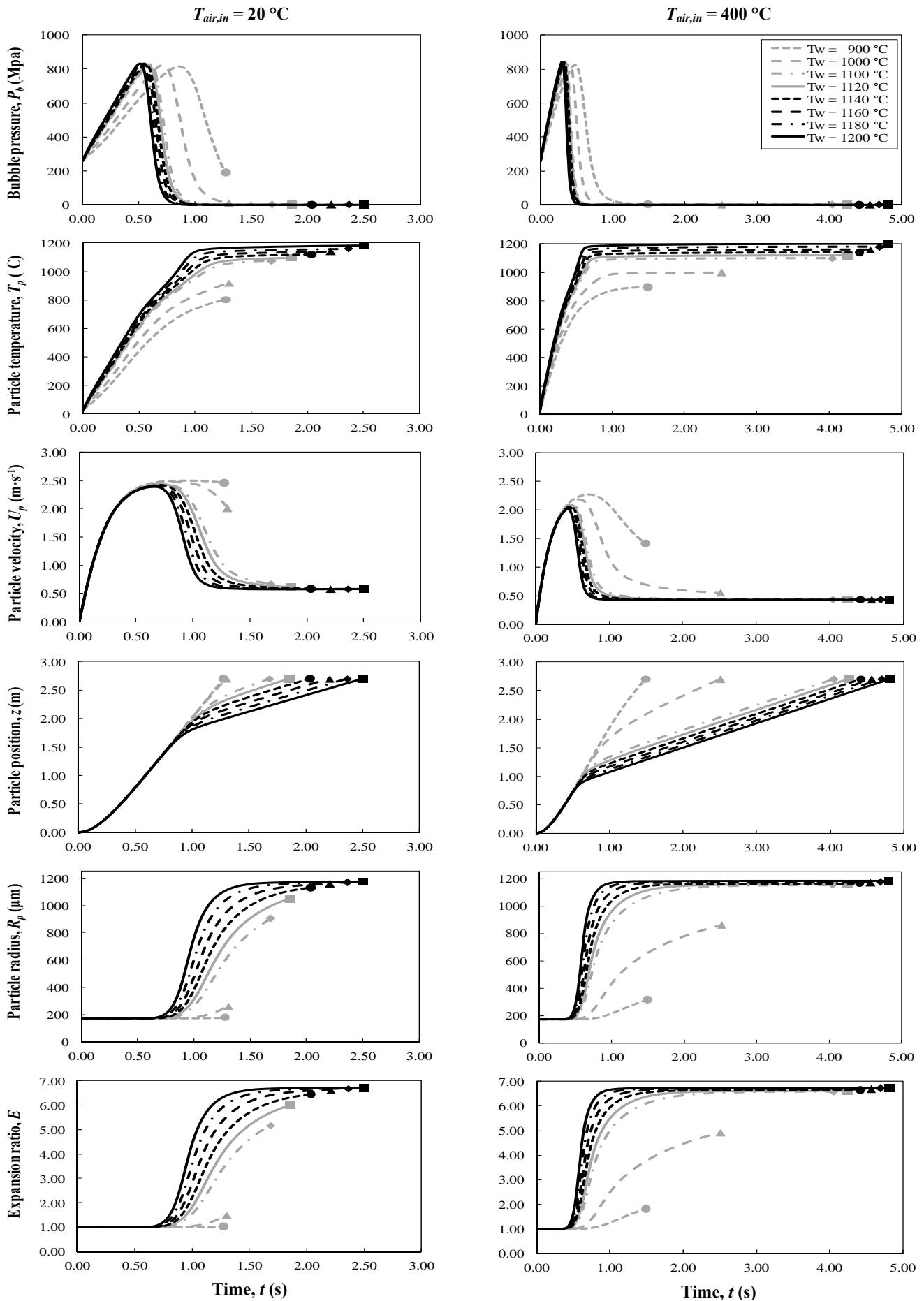


Figure 6. Temporal evolution of particle state variables as a function of heating chamber wall temperature, for the two air feed temperature extremes. Constant parameters:  $\dot{Q}_{air,in} = 50\text{ L}\cdot\text{m}^{-1}$ ,  $D_{p,i} = 350\text{ }\mu\text{m}$ ,  $w_{H_2O,eff} = 2.00\text{ }\%$ .

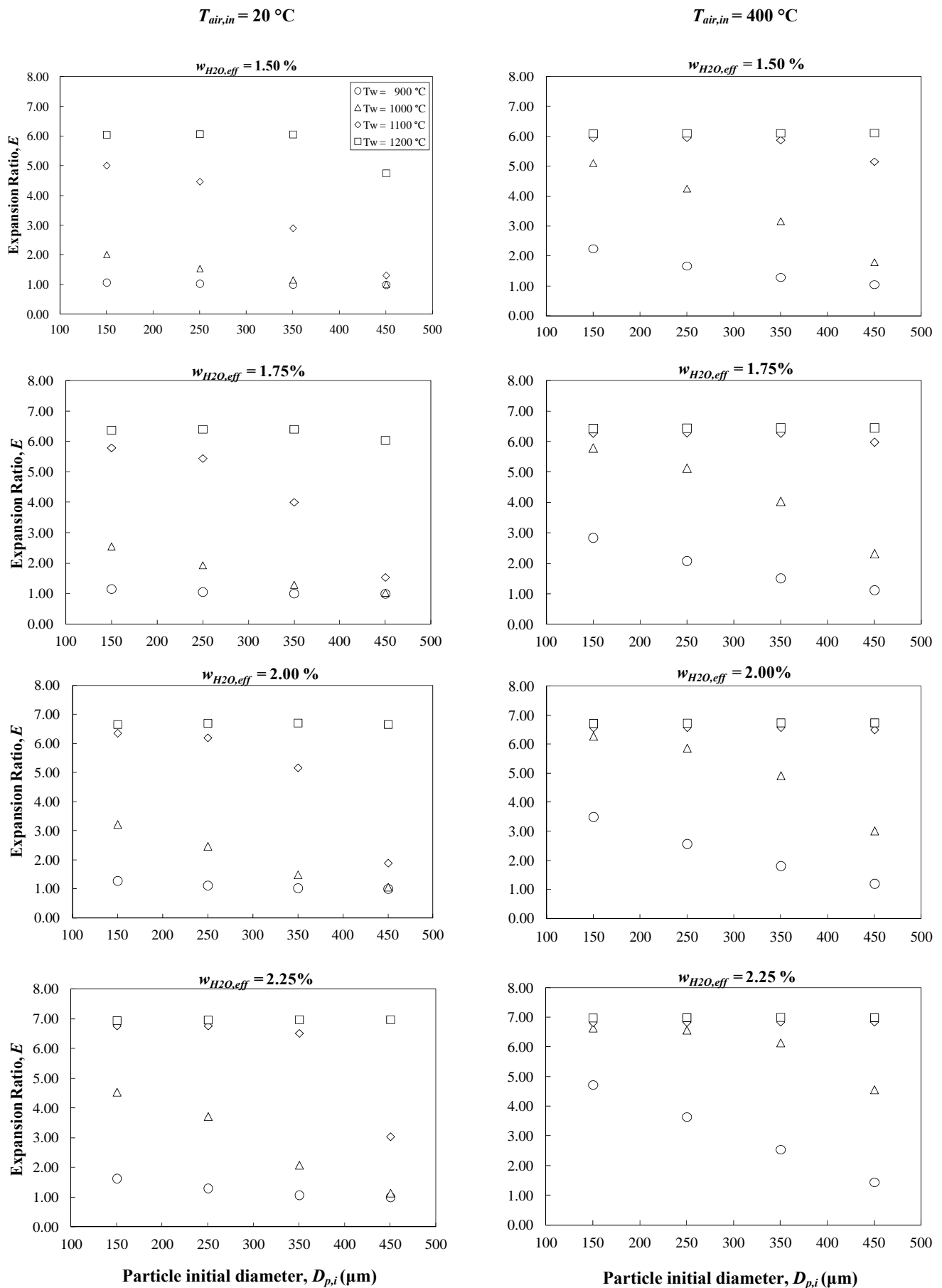


Figure 7. Final perlite particle expansion ratios achieved as a function of heating chamber wall temperature, considering the entire grain size and effective water content ranges. Constant air flow rate:  $\dot{Q}_{air,in} = 50\text{ L}\cdot\text{min}^{-1}$ .



## CONCLUSIONS AND RECOMMENDATIONS

A mathematical model has been developed for perlite grain expansion within a novel vertical electrical furnace. This dynamic model consists of ordinary differential equations for both air and particle heat and momentum balances, as well as nonlinear algebraic equations for air and perlite melt thermophysical properties, probing air as well as particle momentum and heat balances and their effect on perlite acceleration, heating and expansion. The particle heat balance considers heat transfer by convection from/to air and by incident thermal radiation emitted by the internal chamber wall surface, which is heated via independent embedded electrical resistances. The two-phase perlite particle assumption considers an initially minuscule core bubble and an amorphous shell: the entire portion of water available for evaporation is concentrated in the core bubble (effective water content), while the rest is homogeneously dissolved in the melting shell surrounding the bubble (residual water content).

The major conclusion of this modeling study is that the novel vertical electrical furnace design can successfully accomplish perlite expansion up to final product quality standards, within an acceptably wide operating regime. The new vertical electrical furnace enables the precise control of 3 independent process operating parameters (air feed flow rate and temperature, wall temperature) which must be adjusted simultaneously, with in-depth, model-based (not experiential) process understanding to tune perlite expansion successfully. Raw feed as well as furnace operating conditions impact product quality, as shown by model results probing entire parameter ranges.

Raw perlite feedstock thermophysical properties affect perlite expansion efficiency dramatically, indicating that vertical electrical furnace tuning has extreme importance towards high expansion for variable feed grade quality. Figures 6 and 7 corroborate observations derived from novel furnace experimental campaigns: expansion ratio strongly depends on initial particle diameter, perlite origin and chemical composition. Model results imply that feed monodispersity is an ideal prerequisite for high-quality perlite production; actually, optimal operating parameters vary and need be a priori determined for varying perlite ore feeds, especially when production-scale furnaces process batches of variable origin and size distribution. Technical efficiency and economic viability can thus be maximized by raw perlite feed testing and preprocessing.

Raw feed particle size distribution ( $D_{p,i}$ ) is extremely important and must ideally be narrow and monodisperse. Feeds consisting of various size fractions yield poor product quality, due to a wide variety of expansion ratios. Finer particles move slower than coarser ones, because their lower initial mass and radius impact the interplay of weight, drag and buoyancy forces towards inducing a lower terminal velocity compared to coarser grains. Shorter residence times computed for coarser grains in the furnace imply that heating rates may be inadequate, so expansion may not commence or conclude due to unfavourable interplay of gravity, shape and air injection. Moreover, a higher particle mass implies a higher heat amount needed to increase its enthalpy and temperature. Residence time is crucial for coarser particles, whose terminal velocity is higher than that of finer particles: as they travel quicker and contain more water, adequate heating, softening and expansion may not occur until exit. An easy solution is to decrease air flow and/or increase air temperature, as both increase particle residence time.

Effective water content ( $w_{H_2O,eff}$ ) is also a feed physical property affecting perlite expansion and final grain size. Particles with more water tend to expand to higher ratios, even under mild heating (lower furnace temperatures). Low-water raw feeds also require longer residence times.

## ACKNOWLEDGEMENTS

This work has been financed by EU FP7 (CP-IP 228697-2, Efficient exploitation of EU perlite resources for the development of a new generation of innovative and high added value micro-perlite based materials for the chemical, construction and manufacturing industry, EXPERL). Mr. P. Angelopoulos also acknowledges the financial support of the Greek Scholarship Foundation.

## REFERENCES

- Cengel, Y., (2006). Heat Transfer: A Practical Approach (3<sup>rd</sup> edition). New York: McGraw-Hill.
- Chatterjee, K.K. (2008). Uses of Industrial Minerals, Rocks and Freshwater. New York: Nova Science Publishers.
- ElsHEREEF, R., Vlachopoulos, J., Elkamel, A. (2010). Comparison and analysis of bubble growth and foam formation models. Engineering Computations, 27(3), 387-408.
- Giordano, D., Russell, J.K., Dingwell, D.B. (2008). Viscosity of magmatic liquids: A model. Earth and Planetary Science Letters, 271, 123-134.
- Gordon, A.R., Barnes, C. (1932). The entropy of steam and the water-gas reaction. Journal of Physical Chemistry, 36, 1143-1151.
- Gordon, A.R. (1934). Calculation of thermodynamic quantities from spectroscopic data for polyatomic molecules: the free energy, entropy and heat capacity of steam. Journal of Chemical Physics 2, 65-72.
- King, E.G., Todd, S.S., Kelley, K.K. (1948). Perlite Thermal Data and Energy Required for Expansion. Washington DC: United States Bureau of Mines.
- Liang, S.F., Zhu, C. (1998). Principles of Gas-Solid Flows. Cambridge: Cambridge University Press.
- Morsi, S.A., Alexander, A.J. (1972). An investigation of particle trajectories in two-phase flow systems. Journal of Fluid Mechanics, 55, 193-208.
- Papanastassiou, D.J. (1979). Perlite expansion in a vertical furnace – A simplified theoretical analysis. Proceedings of the Perlite Institute Annual Meeting, Dubrovnik, Yugoslavia, 67-71.
- Pai, V., Favelukis, M. (2002). Dynamics of spherical bubble growth. Journal of Cellular Plastics, 38, 403-419.
- Patel, R.D. (1980). Bubble growth in a viscous Newtonian liquid. Chemical Engineering Science, 35, 2352-2356.
- Proussevitch, A.A, Sahagian, D.L. (1998), Dynamics and energetics of bubble growth in magmas: Analytical formulation and numerical modeling, Journal of Geophysical Research, 103(B8), 18223-18252.
- Schiller, L., Nauman, A., (1933), Über die grundlegende Berechnung bei der Schwebkrauffbereitung, Zeitschrift des Vereins Deutscher Ingenieure, 44, 318-320.
- Shackley, D. (1988), Characterization and Expansion of Perlite, PhD Thesis. University of Nottingham, UK.
- Zahringer, K., Martin, J.-P., Petit, J.P. (2001), Numerical simulation of bubble growth in expanding perlite, Journal of Materials Science, 36(11), 2691-2705.